© 2016. Published by The Company of Biologists Ltd | Journal of Experimental Biology (2016) 219, 2763-2773 doi:10.1242/jeb.141721

RESEARCH ARTICLE

High rates of glucose utilization in the gas gland of Atlantic cod (*Gadus morhua*) are supported by GLUT1 and HK1b

Kathy A. Clow[1], Connie E. Short[1], Jennifer R. Hall[2], Robert L. Gendron[3], Hélène Paradis[3], Ankur Ralhan[3] and William R. Driedzic[1,*]

ABSTRACT

The gas gland of physoclistous fish utilizes glucose to generate lactic acid that leads to the off-loading of oxygen from haemoglobin. This study addresses characteristics of the first two steps in glucose utilization in the gas gland of Atlantic cod (*Gadus morhua*). Glucose metabolism by isolated gas gland cells was 12- and 170-fold higher, respectively, than that in heart and red blood cells (RBCs) as determined by the production of ^3H_2O from [2-^{3}H] glucose. In the gas gland, essentially all of the glucose consumed was converted to lactate. Glucose uptake in the gas gland shows a very high dependence upon facilitated transport as evidenced by saturation of uptake of 2-deoxyglucose at a low extracellular concentration and a requirement for high levels of cytochalasin B for uptake inhibition despite the high efficacy of this treatment in heart and RBCs. Glucose transport is via glucose transporter 1 (GLUT1), which is localized to the glandular cells. GLUT1 western blot analysis from whole-tissue lysates displayed a band with a relative molecular mass of 52 kDa, consistent with the deduced amino acid sequence. Levels of 52 kDa GLUT1 in the gas gland were 2.3- and 33-fold higher, respectively, than those in heart and RBCs, respectively. Glucose phosphorylation is catalysed by hexokinase Ib (HKIb), a paralogue that cannot bind to the outer mitochondrial membrane. Transcript levels of HKIb in the gas gland were 52- and 57-fold more abundant, respectively, than those in heart and RBCs. It appears that high levels of GLUT1 protein and an unusual isoform of HKI are both critical for the high rates of glycolysis in gas gland cells.

KEY WORDS: Glucose metabolism, Heart, RBC, [2-^{3}H]glucose, Facilitated transport

INTRODUCTION

The swim bladder of many teleost fish functions to regulate buoyancy. In physoclistous fish, the swim bladder does not vent to the atmosphere; in these species, the swim bladder is filled primarily with oxygen via a gas gland. This tissue consists of glandular cells that cluster around a rete mirabile. The glandular cells generate lactic acid with protons accumulating via counter-current exchange at the tip of the rete. The low pH associated with lactate production in turn causes oxygen to unload via the Bohr and Root effects and oxygen moves by diffusion from the blood into the swim bladder (Pelster, 1997, 2015).

Lactate is produced from glucose either through the glycolytic pathway or via the pentose phosphate pathway, which is quite active in gas gland tissue (Pelster, 1997, 2015). In European eel (*Anguilla anguilla*) and American eel (*Anguilla rostrata*), 60–80% of the glucose taken up by the gas gland is converted to lactate (Pelster et al., 1989, 1994; Pelster and Scheid, 1993), whereas, in isolated gas gland cells from Atlantic cod (*Gadus morhua*), more lactate is produced than could be accounted for by the rate of glucose metabolism (Hall et al., 2014). The production of lactate as a metabolic end product is consistent with low mitochondrial density, poorly developed cristae, and low levels of cytochrome oxidase and citric acid cycle enzymes in the gas gland (Copeland, 1969; Boström et al., 1972; Morris and Albright, 1975; Ewart and Driedzic, 1990; Pelster and Scheid, 1991; Walsh and Milligan, 1993). Although much is known about the neural control of gas secretion (Nilsson, 2009) and H^+ transfer mechanisms (Pelster, 2004; Umezawa et al., 2012), very little is understood about the initial stages of glucose utilization. This study addresses this issue in the gas gland of Atlantic cod.

We measured metabolism in isolated gas gland cells with the objective of assessing the relative importance of facilitated glucose transport for glucose entry and the phosphorylation of glucose, the first enzyme-catalysed reaction in glucose utilization. The maximal rate of glucose uptake was assessed by tracking the initial uptake of 2-deoxyglucose (2-DG) and steady-state metabolism of glucose was determined by tracking the release of ^3H_2O from [2-^{3}H]glucose. The latter approach measures the summed rate of glycolysis and the pentose phosphate pathway (Hutton, 1972). Rates of uptake and steady-state metabolism were compared with transcript and protein levels of glucose transporter 1 (GLUT1) and hexokinase I (HKI).

Glucose enters cells either by simple diffusion or by facilitated transport via GLUTs. There are four major sodium-independent proteins (GLUT1–4) that show tissue-specific distribution (Mueckler and Thorens, 2013; Chen et al., 2015). In Atlantic cod gas gland and heart, *GLUT1* constitutes greater than 95% and in RBCs greater than 85% of the relative quantity of mRNA for this class of glucose transporter (Hall et al., 2014). As such, is it likely that GLUT1 protein is the major vehicle for facilitated glucose transport in these tissues. A *GLUT1* orthologue is also a major transcript in the swim bladder of torafugu (*Takifugu rubripes*) and *in situ* hybridization has revealed its presence in gas gland cells but not rete mirabile (Munakata et al., 2012). There is a linear relationship between glucose metabolism of isolated cells and the relative quantity of *GLUT1* mRNA in gas gland, heart and RBCs (Hall et al., 2014), suggesting that GLUT1 protein is a major determinant of glucose utilization. Here, we assessed the importance of facilitated glucose transport and, additionally, the localization and size of GLUT1 protein.

[1]Department of Ocean Sciences, Ocean Sciences Centre, Memorial University of Newfoundland, St John's, NL, Canada A1C 5S7. [2]Aquatic Research Cluster, CREAIT Network, Memorial University of Newfoundland, St John's, NL, Canada A1C 5S7. [3]Division of BioMedical Sciences, Faculty of Medicine, Memorial University, St John's, NL, Canada A1B 3V6.

*Author for correspondence (wdriedzic@mun.ca)

W.R.D., 0000-0002-4105-1766

Received 11 April 2016; Accepted 28 June 2016

Journal of Experimental Biology (2016) 219, 2763-2773 doi:10.1242/jeb.141721

Once glucose enters the cell it is phosphorylated to glucose 6-phosphate (G6P) by HK. In mammals, HK exists in two major isoforms: HKI and HKII. HKI binds to mitochondria and is considered to couple the use of glucose to oxidative metabolism. HKII shows both cytoplasmic and mitochondrial localization, may be more important in anabolic pathways and directing G6P to the pentose shunt pathway, and is found primarily in insulin-sensitive tissues (Mandarino et al., 1995; Wilson, 2003; Calmettes et al., 2013). The cDNAs for two *HKI* paralogues (*HKIa* and *HKIb*) were cloned from Atlantic cod (Hall et al., 2009). HKIa transcripts are expressed primarily in heart and brain; *HKIb* transcripts are ubiquitously expressed, with the highest levels in brain, gill, kidney and spleen. *HKIb* is an unusual paralogue in that in the 15 amino acid N-terminal domain, required for mitochondrial binding, there is a substitution of isoleucine for leucine at site 7 (Hall et al., 2009). As a conserved sequence is required for binding of HK to the outer mitochondrial membrane (Gelb et al., 1992; Sui and Wilson, 1997), although not proven, it is likely that HKIb does not bind to mitochondria in a similar fashion to that of other HKIs. The gas gland was not assessed in the report of Hall et al. (2009). High *in vitro* activity of total HK appears to be a hallmark of gas gland metabolism. HK activity is substantially higher in gas gland than in skeletal muscle in Atlantic cod (Boström et al., 1972) and European eel (Pelster and Scheid, 1991). In addition, in Atlantic cod, HK activity in the gas gland (Ewart and Driedzic, 1990) appears to be about 4-fold higher than that in heart (Hansen and Sidell, 1983). Here, we report levels of *HKI* transcripts and HK activity in gas gland, heart and RBCs.

MATERIALS AND METHODS

Animal source and husbandry

Hatchery-reared Atlantic cod (*Gadus morhua* Linnaeus 1758) were obtained from the Dr Joe Brown Aquatic Research Building at the Ocean Sciences Centre, Memorial University of Newfoundland. Fish were held indoors in free-flowing seawater between 8 and 10°C, exposed to a natural photoperiod with fluorescent lights set by an outdoor photocell, and fed daily with a commercial diet (Shur-Gain, Truro, NS, Canada). Body mass was 869±153 g. On the day of the experiment, approximately 1–3 ml of blood was collected from the caudal vessel with a heparinized syringe and kept on ice until cell preparations were completed. Fish were then killed with a sharp blow to the head and gas glands quickly excised for the isolation of cells. In experiments including heart cells, the heart was excised first, followed by isolation of the gas gland. In the transcript analysis study, tissues were flash frozen in liquid nitrogen and stored at −80°C. Animal protocols were approved by the Institutional Animal Care Committee, Memorial University of Newfoundland, St John's, NL, Canada.

Experimental overview

Four general experiments were conducted involving isolated gas gland cells: (i) measurement of the rate of uptake of 2-DG; (ii) establishment of the linearity of glucose metabolism from the production of ^3H_2O; (iii) assessment of the importance of facilitated glucose transport; and (iv) investigation of the relationship between rates of glucose metabolism and levels of GLUT1 and HK.

Preparation of gas gland cells, myocytes and RBCs

The gas gland was generally isolated by opening the swim bladder, scraping the desired tissue off the bladder wall and severing any connective tissue/vessels. The gas gland was minced finely in a watch glass with 5 ml of enzyme mixture containing 0.5 mg ml^{-1} BSA, 0.3 U ml^{-1} collagenase (type 4), 0.3 U ml^{-1} protease, 70 U ml^{-1} DNase and 3.9 U ml^{-1} elastase in incubation medium (mmol l^{-1}: 155 NaCl, 5 KCl, 1 NaH_2PO_4, 2 $MgSO_4$, 2 $CaCl_2$, 10 Hepes and 5 glucose, adjusted to pH 7.6). Protease was purchased from Sigma while the other enzymes were purchased from Worthington Biochemical Corp. The minced gas gland was gently agitated continuously by pipetting up and down with a plastic Pasteur pipette for 10 min. This mixture was put through a 70 µm filter resting on a 50 ml centrifuge tube containing 20 ml of incubation medium and 2% BSA. The remaining undigested tissue left on the filter was put back onto the watch glass and the enzyme incubation/filtration procedure was repeated twice. Cells were centrifuged at 100 ***g*** for 5 min. The medium was poured off, and the cells were washed twice with incubation medium. Cells were centrifuged for a final time and resuspended to a concentration of 25–50 mg cells ml^{-1}.

Atlantic cod myocytes were prepared using a perfusion system as described in Hall et al. (2014). Briefly, a retrograde perfusion of the heart was performed at 8°C, first with an isolating solution for 8 min and then with an enzyme solution for 12–14 min. Following the enzymatic digestion, the atrium was removed from the ventricle, and the ventricle was cut into small pieces and then gently agitated using the opening of a plastic Pasteur pipette. The isolated cells were passed through a 150 µm filter and centrifuged at 200 ***g*** for 5 min, and the cell pellet was weighed. Cells were resuspended in incubation medium. In order to protect myocytes from calcium overloading, Ca^{2+} was added back to the suspension to a final concentration of 2 mmol l^{-1} in five increments over a period of 25 min. Myocytes were resuspended to a final concentration of 50 mg ml^{-1}.

RBCs were isolated from the initial blood sample collected prior to the collection of the gas gland and were washed and isolated according to Driedzic et al. (2013). RBCs were resuspended to a final concentration of 50 mg ml^{-1}.

Uptake of 2-DG

A 200 µl sample of the gas gland cell suspension was added to 16×100 mm glass tubes containing [2-^{3}H]deoxy-D-glucose (11kBq; Perkin Elmer, Woodbridge, ON, Canada), [^{14}C]mannitol (3.7kBq; Perkin Elmer) and 5 mmol l^{-1} 2-DG. Cells were incubated for 1, 2, 3, 4, 5, 7.5, 10, 15, 20, 30 and 60 min at 8°C. After each time point, the sample was spun at 6000 ***g*** for 30 s; 150 µl of the supernatant was added to a vial with scintillation fluid and the remaining supernatant was discarded; 100 µl of 6% perchloric acid was added to the cell pellet and the lysate centrifuged at 10,000 ***g*** for 5 min. Both the supernatant from the first spin and from the cell pellet were counted with a dual-labelled program for both ^{3}H and ^{14}C using a Packard 2500TR liquid scintillation counter (PerkinElmer). Extracellular space, using [^{14}C]mannitol, and the intracellular concentration of 2-DG (µmol g^{-1}) were calculated as previously described (Rodnick et al., 1997). Uptake of 2-DG by gas gland cells incubated with 0.01, 0.025, 0.05, 0.075, 0.1, 0.175, 0.25, 0.5, 1 or 2.5 mmol l^{-1} of extracellular 2-DG was also tested as described above. In this experiment, incubations were stopped at 5 min.

In a separate experiment, the ratio of free intracellular 2-DG to 2-deoxyglucose 6-phosphate (hereafter 2-DGP) was determined by incubating gas gland cells, as described above, in either 0.5 or 5 mmol l^{-1} 2-DG for 5 min at 8°C. Cell pellets were lysed by the addition of 200 µl water, and spun at 10,000 ***g*** for 5 min; 50 µl of the supernatant was counted directly while a 100 µl aliquot was added to a DEAE-Sephacel column. Successive washes of distilled water and 0.2 mmol l^{-1} HCl were used to elute 2-DG and 2-DGP,

Journal of Experimental Biology (2016) 219, 2763-2773 doi:10.1242/jeb.141721

respectively. Aliquots of the cell extract and both column fractions were counted for radioactivity.

Glucose metabolism and lactate production

The procedure for determining glucose metabolism in gas gland cells was similar to that used previously with isolated RBCs (Driedzic et al., 2014); 200 µl of a 25–50 mg ml^{-1} cell suspension was incubated in 16×100 mm glass tubes containing [2-^{3}H]glucose (7.4kBq; American Radiolabeled Chemicals, Burnaby, Canada). Cell suspensions containing 5 mmol l^{-1} glucose were incubated for 1, 2 and 3 h at 8°C; 5 mmol l^{-1} is within the physiological range for this population of cod (Driedzic et al., 2013, 2014). After each time point, the sample was centrifuged at 10,000 ***g*** for 30 s; the supernatant was collected and frozen. Glucose metabolism was measured by the ^3H_2O produced from [2-^{3}H]glucose during the incubation period. ^3H_2O was separated from the [2-^{3}H]glucose in the supernatant using chromatography as previously described (Driedzic et al., 2013). Fractions containing ^3H_2O were counted. Background counts (time zero) were obtained by adding the label to a 200 µl aliquot of cell suspension, centrifuging immediately and flash freezing the supernatant. These counts were subtracted from all time points.

Lactate was measured in the supernatant collected after each time point. The supernatant was deproteinized 1:1 with 6% perchloric acid and 25–50 µl of extract was added to an assay medium containing glycine buffer (Sigma, G5418) and 2.5 mmol l^{-1} NAD^+, pH 9.0 at room temperature. Samples were read after 10 min before adding 30 IU ml^{-1} lactate dehydrogenase. Absorbance was read for another 60 min or until stable with a DTX 880 microplate reader (Beckman Coulter, Mississauga, ON, Canada).

Glucose metabolism in gas gland cells was assessed at extracellular glucose concentrations of 0.313, 0.5, 0.625, 1.25, 2.5, 5, 10, 15 and 20 mmol l^{-1} in the incubation medium at 8°C. After 2 h, the incubation was terminated and glucose metabolism was measured as described above. Background counts were obtained as described above except the cell suspension contained 10 mmol l^{-1} of extracellular glucose.

The effect of 25 µmol l^{-1} cytochalasin B, a glucose transport inhibitor, on glucose metabolism in gas gland cells was tested. Thirty minutes prior to the addition of [2-^{3}H]glucose, cytochalasin B was added to the cell suspension containing 0.5, 2.5, 5 or 10 mmol l^{-1} extracellular glucose. Because cytochalasin B was dissolved in 0.33% DMSO, cells were also incubated with DMSO in incubation medium containing 0.5 and 10 mmol l^{-1} glucose. In a second cytochalasin B experiment, various concentrations of cytochalasin B were used to measure the percentage inhibition of glucose metabolism in gas gland, myocytes and RBCs. Cytochalasin B at 25, 50, 100 or 200 µmol l^{-1} was added to the cell suspension containing 5 mmol l^{-1} extracellular glucose 30 min before the addition of the isotope. After 2 h, the incubation was terminated and glucose metabolism was measured as described above.

HK activity assays

Cell pellets were sonicated in 4 volumes of ice-cold extraction buffer containing 50 mmol l^{-1} imidazole and 1 mmol l^{-1} EDTA, pH 7.4 at 4°C. For measurement of HK enzyme activity, an aliquot of the homogenate was further diluted 1:10, 1:5 and 1:2 for gas gland, heart and RBCs, respectively. HK assays included (in mmol l^{-1}): 50 imidazole buffer, 0.4 $NADP^+$, 5 $MgCl_2$ and 1 glucose, with 2 U ml^{-1} G6P dehydrogenase. The reaction was initiated by the addition of 5.0 mmol l^{-1} ATP. Control rates were determined simultaneously in separate wells without the addition of ATP. Reactions were carried out at 340 nm using a SpectraMax M5 microplate reader (Molecular Devices, Sunnyvale, CA, USA), with reaction rate calculated based on an extinction coefficient of 6.22 for NADPH.

Transcript analysis

Total RNA was extracted using TRIzol Reagent (Invitrogen/Life Technologies, Burlington, ON, Canada). Cells were homogenized in TRIzol Reagent using a motorized Kontes RNase-Free Pellet Pestle Grinder (Kimble Chase, Vineland, NJ, USA). The remainder of the protocol was carried out following the manufacturer's instructions. Total RNA was treated with TURBO DNA-free (Ambion/Life Technologies) following the manufacturer's instructions. RNA integrity was verified by 1% agarose gel electrophoresis and purity was assessed by A_{260}/A_{280} and A_{260}/A_{230} UV NanoDrop spectrophotometry.

First-strand cDNA was synthesized from 1 µg of DNaseI-treated total RNA in a 20 µl reaction using random primers (250 ng; Invitrogen/Life Technologies) and M-MLV reverse transcriptase (200 U; Invitrogen/Life Technologies) with the manufacturer's first strand buffer (1× final concentration) and DTT (10 mmol l^{-1} final concentration) at 37°C for 50 min.

qPCR analyses were performed using the ViiA 7 Real-Time PCR system (Applied Biosystems/Life Technologies). The 96-well platform was used for primer quality and normalizer testing and the 384-well platform was used for the experimental plate. In all cases, the reaction volume for the PCR amplifications was 13 µl and contained 1× Power SYBR Green PCR Master Mix (Applied Biosystems/Life Technologies), 50 nmol l^{-1} of both the forward and reverse primers, and the indicated cDNA quantity (see below). The real-time analysis program consisted of 1 cycle of 50°C for 2 min, 1 cycle of 95°C for 10 min and 40 cycles of 95°C for 15 s and 60°C for 1 min, with fluorescence detection at the end of each 60°C step.

The sequences of all primer pairs used in qPCR analyses are presented in Table 1. Primer sequences were based on the following sequences from GenBank: *GLUT1* (AY526497), *HKIa* (EU053127), *HKIb* (EU053128), 40S ribosomal protein S28 gene (ES771075) and 60S ribosomal protein L34 gene (FG319319). Each primer pair was quality tested to ensure that a single product was amplified (dissociation curve analysis) and that there was no primer-dimer present in the no-template control. Amplicons were electrophoretically separated on 2% agarose gels and compared with a 1 kb plus ladder (Invitrogen/Life Technologies) to verify that the correct sized fragment was being amplified. Amplification efficiencies (Pfaffl, 2001) were calculated using cDNA synthesized from gas gland, heart and RBCs from an individual fish. The reported efficiencies are an average of the three values. Standard curves were generated using a 5-point 1:3 dilution series starting with cDNA representing 10 ng of input total RNA.

Transcript levels of the genes of interest (GOI) were normalized to two endogenous control genes. To select these endogenous controls, transcript levels were measured for 18 candidate normalizers using cDNA representing 5 ng of input total RNA synthesized from gas gland, heart and RBCs, from the same specimen used above, as templates (data not shown). The four most stably expressed transcripts were then analysed using cDNA representing 5 ng of input total RNA synthesized from gas gland, heart and RBCs from four fish. Ct values were analysed using geNorm to select the most stably expressed transcripts. Using this software, 40S ribosomal protein S28 and 60S ribosomal protein L34

Journal of Experimental Biology (2016) 219, 2763-2773 doi:10.1242/jeb.141721

Table 1. Primers used in qPCR studies

Gene name	Direction	Nucleotide sequence (5′–3′)	Efficiency (%)*	Amplicon size (bp)
GLUT1	Forward	GTGTTTGGCATCGAGTCCTT	100	143
	Reverse	TCGTTCTTGTTGAGCAGCAG		
HKIa	Forward	CGTCACCTGGACCAAGAAGT	97	108
	Reverse	ATGATGTCCGCCTCGTAGTC		
HKIb	Forward	GAGGGCTATCTGCTGACCTG	98	97
	Reverse	CTCGCTTCTTAATGGCCTTG		
40S ribosomal protein S28	Forward	CCCTTCACGTTCCTGATGAT	95	115
	Reverse	AGCTTGCCAGAGTCACCAAG		
60S ribosomal protein L34	Forward	CAACACTGCCTCCAACAAGA	88	121
	Reverse	CAGTCTCCCTGGGCAGATAC		

*Amplification efficiencies were calculated using a 5-point 1:3 dilution series starting with cDNA representing 10 ng of input RNA. See Materials and methods for details.

(geNorm M=0.33 for both genes) were determined to be the most stable.

Transcript (mRNA) expression levels of the GOI (*GLUT1*, *HKIa* and *HKIb*) were then assessed by qPCR. In all cases, cDNA representing 5 ng of input RNA was used as a template in the PCR reactions. On each plate, for every sample, the GOI and endogenous controls were tested in triplicate and a no-template control was included. The relative quantity (RQ) of each transcript was determined using the ViiA 7 Software Relative Quantification Study Application (version 1.2.3; Applied Biosystems/Life Technologies), with normalization to 40S ribosomal protein S28 and 60S ribosomal protein L34 transcript levels, and with amplification efficiencies incorporated. For each GOI, the sample with the lowest normalized expression (mRNA) level was set as the calibrator sample (i.e. assigned an RQ value of 1).

GOI expression was further analysed to measure transcript levels on a per gram of tissue basis. The GOI mRNA level measured in the qPCR reaction was based upon 5 ng of cDNA (corresponding to 5 ng of input RNA). The normalized GOI mRNA level was multiplied by 200 to generate the GOI mRNA level per µg of total RNA. Next, the quantity of total RNA (µg) generated from the TRIzol extraction(s) was calculated by multiplying the RNA concentration (µg µl^{-1}) by the resuspension volume (100 µl). This value was then divided by the mass of tissue (g) used in the RNA extraction(s) to calculate the quantity (µg) of total RNA per mass (g) of tissue. Finally, the GOI mRNA level per mass (µg) of total RNA was multiplied by the quantity (µg) of total RNA per mass (g) of tissue to generate the GOI mRNA level per mass (g) of tissue. The sample with the lowest detectable normalized quantity (mRNA level g^{-1} tissue) of that particular GOI was set as the calibrator.

Histology and immunohistochemistry

For histological studies, the gas gland was lifted off the swim bladder wall (as opposed to scraping) and any connective tissue was severed. Gas glands were frozen in OCT embedding compound. Frozen sections of 7 µm were prepared using a Leica CM1900 cryostat. Haematoxylin and eosin histological staining was performed on some sections and immunohistochemistry on other sections. For immunohistochemistry, sections were post-fixed in 4% paraformaldehyde in phosphate-buffered saline for 20 min at room temperature and then washed in TBS (10 mmol l^{-1} Tris-HCl, pH 7.6, and 150 mmol l^{-1} NaCl). Samples were then blocked in 2% ECL Prime Blocking Agent (GE Healthcare, KPL, Gaithersburg, MD, USA) in TBS for 1 h at room temperature. Incubations with antibodies were performed overnight in blocking agent in buffer at room temperature. Antibodies used were mouse monoclonal IgG2b anti-GLUT1 antibody (MAB1418, R&D Systems) at 20 µg ml^{-1} or an isotype-matched control mouse monoclonal IgG2b anti-His antibody (R930-25, Invitrogen) at the same concentration. Sections

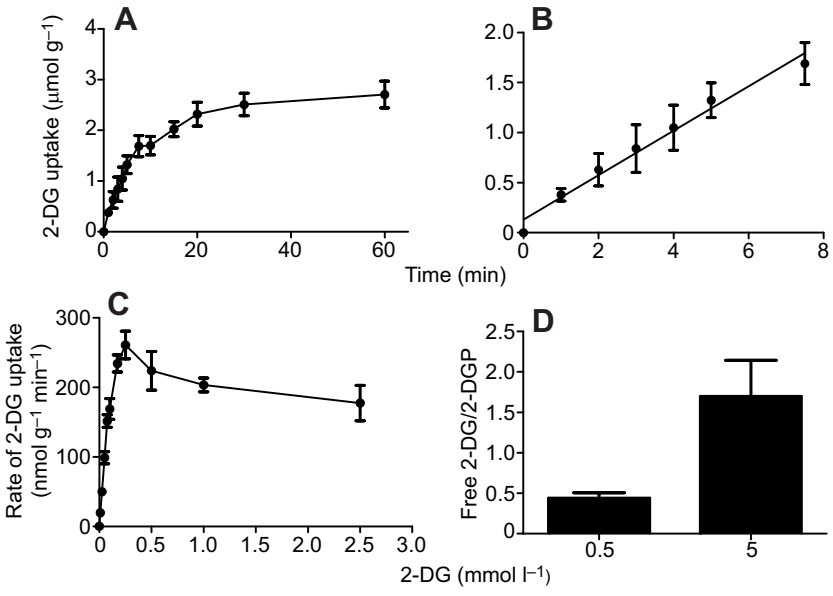

Fig. 1. Uptake of 2-deoxyglucose (2-DG) by gas gland cells isolated from Atlantic cod and ratio of free intracellular 2-DG/2-DG phosphate (2-DGP). (A) Uptake of 2-DG by gas gland cells incubated in 5 mmol l^{-1} extracellular 2-DG over 1 h at 8°C. N=4 for values at 0, 5, 10, 15, 30 and 60 min; N=3 for the other time points. (B) Uptake of 2-DG by gas gland cells incubated in 5 mmol l^{-1} extracellular 2-DG for up to 7.5 min at 8°C. Data are taken from A and were analysed by linear regression (y=0.22x+0.13, r^2=0.98; P<0.0001). N=4 for the value at 5 min; N=3 for the other time points. (C) Rate of 2-DG uptake by gas gland cells incubated in various concentrations of extracellular 2-DG for 5 min at 8°C. Sample sizes for the different concentrations of 2-DG (mmol l^{-1}) were as follows: 0, N=5; 0.01, N=4; 0.025, N=3; 0.05, N=3; 0.075, N=3; 0.1, N=5; 0.175, N=3; 0.25, N=4; 0.5, N=3; 1, N=3; and 2.5, N=3. (D) Ratio of free 2-DG to 2-DGP following 5 min of incubation with an extracellular 2-DG concentration of either 0.5 or 5 mmol l^{-1}. N=8.

Journal of Experimental Biology (2016) 219, 2763-2773 doi:10.1242/jeb.141721

were developed using appropriate secondary alkaline phosphatase (AP)-conjugated antibody (Jackson ImmunoResearch) and Vector Red AP substrate with Levamisole to block endogenous AP activity (Vector Laboratories Inc.). Sections were photographed using a Leica light microscope fitted with a Q Imaging digital camera and Openlab software.

GLUT1 western blotting and protein quantification

Protein lysate from RF/6A, Rhesus macaque choroid-retina (American Type Culture Collection, Manassas, VA, USA) endothelial cell line and Atlantic cod tissues (gas gland, heart and RBCs) for western blot analyses were prepared in Triton lysis buffer [50 mmol l^{-1} Tris-HCl, pH 7.6, 150 mmol l^{-1} NaCl, 0.5% (w/v) sodium deoxycholate, 0.1% (w/v) SDS, 1% (v/v) Triton X-100 and 10% (v/v) glycerol] supplemented with 1 mmol l^{-1} dithiothreitol, 10 µg ml^{-1} leupeptin, 0.3 U ml^{-1} aprotinin, 1 mmol l^{-1} phenylmethylsulfonyl fluoride, 1 mmol l^{-1} sodium orthovanadate, 50 mmol l^{-1} sodium fluoride and 25 mmol l^{-1} ß-glycerophosphate as previously described (Paradis et al., 2008). Tissues were homogenized and cell and tissue lysates were clarified by centrifugation; protein concentration was determined by the Bio-Rad Protein Assay kit (Bio-Rad Laboratories, Hercules, CA, USA) using bovine serum albumin (BSA) as the standard. Protein lysates were loaded onto an SDS-PAGE gel and transferred to nitrocellulose membrane (Bio-Rad Laboratories) for western blot analysis or stained with Coomassie Blue R-250.

For GLUT1 western blots, nitrocellulose membranes were preincubated for 1 h at 55°C in 2% ECL Prime Blocking Reagent (GE Healthcare) in TBST (TBS with 0.05% Tween 20). Blots were washed 3 times with TBST and incubated with the GLUT1 antibody described above (2 µg ml^{-1}) in 5% BSA (MP Biomedicals, LLC, Solon, OH, USA) in TBST at room temperature. GLUT1 signal was revealed using Chemiluminescence ECL Prime detection reagents (GE Healthcare) and a Kodak Gel Logic 2200 imaging system (Eastman Kodak Company, Rochester, NY, USA) with Carestream Molecular imaging software (Woodbridge, CT, USA). Protein expression signals were quantified by densitometry.

Data analysis

Values are expressed as means±s.e.m. Data were analysed with GraphPad Prism. Statistical tests applied are given in the legends to figures. Unless otherwise stated, all data sets subjected to statistical analysis passed a normality test. In all cases, $P<0.05$ was considered to be significant.

RESULTS

Uptake of 2-DG

The uptake of 2-DG with respect to time by isolated gas gland cells followed the expected pattern of rapid accumulation with saturation once equilibration of the radiotracer between the extracellular space and intracellular water was achieved (Fig. 1A). Initial uptake was linear for at least 7.5 min ($y=0.22x+0.13$, $r^2=0.98$; Fig. 1B); as such, a 5 min incubation period was utilized in further experiments with 2-DG. The uptake of 2-DG saturated with respect to concentration, indicative of a facilitated transport process (Fig. 1C). According to Michaelis–Menten kinetics, assessed by non-linear regression, the V_{max} was 237±23 nmol g^{-1} min^{-1} with a K_m of 0.05± 0.02 mmol l^{-1}.

At sub-physiological concentrations of extracellular substrate (0.5 mmol l^{-1} 2-DG), the level of 2-DGP exceeded that of free intracellular 2-DG, indicating that the rate of phosphorylation via HK exceeded uptake (Fig. 1D). At physiological levels of substrate (5 mmol l^{-1} 2-DG), the level of free 2-DG exceeded that of 2-DGP (2-DG/2-DGP=1.7), indicating that the rate of uptake exceeded that of phosphorylation (Fig. 1D) under these short-term conditions.

Initial studies of glucose metabolism and lactate production by uninhibited gas gland cells

Glucose metabolism was assessed by monitoring the rate of ^3H_2O production from [2-^{3}H]glucose. This approach measures the net outcome of uptake and the capacity to metabolise glucose. Both glucose metabolism ($y=9.79x+1.42$, $r^2=0.99$) and lactate production ($y=26x+75$, $r^2=99$) were linear for at least 3 h (Fig. 2A,B). Rates of glucose metabolism and lactate production were 163 and 437 nmol g^{-1} cells min^{-1}, respectively (Fig. 2C). The ratio of lactate production to glucose metabolism, based on individual experiments, was 2.76±0.49, a value that is not significantly different from 2 (one-sample *t*-test).

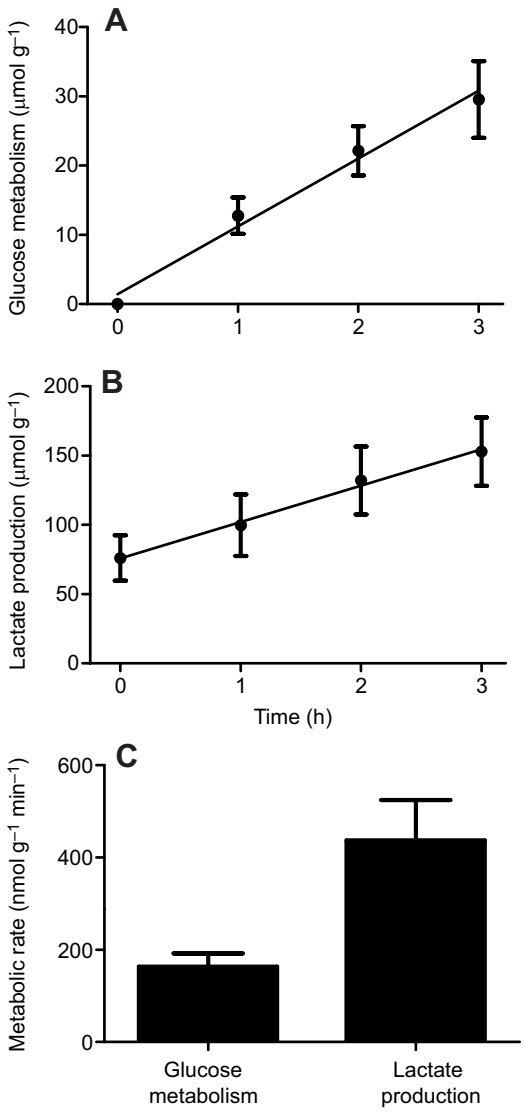

Fig. 2. Glucose metabolism and lactate production by gas gland cells isolated from Atlantic cod. Cells were incubated in 5 mmol l^{-1} extracellular glucose over 3 h at 8°C. (A) Glucose metabolism of isolated gas gland cells measured by ^3H_2O production from [2-^{3}H]glucose. Data were analysed by linear regression ($y=9.79x+1.42$, $r^2=0.99$, $P=0.0075$). (B) Lactate production by isolated gas gland cells. Data were analysed by linear regression ($y=26.2x+75.8$, $r^2=0.99$, $P=0.003$). (C) Rates of glucose metabolism and lactate production over 3 h calculated for individual experiments. $N=5$ in all cases.

Journal of Experimental Biology

Journal of Experimental Biology (2016) 219, 2763-2773 doi:10.1242/jeb.141721

Based on the time course experiment, an incubation time of 2 h was selected for further studies with [2-^{3}H]glucose (Fig. 2A). Glucose metabolism was assessed at different levels of extracellular glucose (Fig. 3). Metabolism increased as concentration was elevated until a saturating level was reached. According to Michaelis–Menten kinetics, the V_{max} was 262± 17 nmol g^{-1} min^{-1} with a K_m of 0.9±0.27 mmol l^{-1}.

Inhibition of metabolism by cytochalasin B

The impact on glucose metabolism of 25 µmol l^{-1}cytochalasin B was determined initially. Average rates of glucose metabolism were decreased in the presence of cytochalasin B at all extracellular concentrations of glucose and significantly so at 2.5 and 10 mmol l^{-1} (Fig. 4). At a glucose concentration of 5 mmol l^{-1}, the average level of inhibition of metabolism was 23%. The decrease in glucose metabolism was less than expected given what appeared to be a large facilitated transport component based on the saturation of 2-DG uptake and the high rates of glucose metabolism relative to other tissues (Hall et al., 2014). This motivated us to examine the relationship between glucose metabolism and the concentration of cytochalasin B in the gas gland, heart and RBCs. As expected from earlier studies, the rate of glucose metabolism in the gas gland was substantially higher than that of myocytes or RBCs (Fig. 5A,C,E, with no cytochalasin B). Cytochalasin B inhibited glucose metabolism in all cell types but the relationship to extracellular inhibitor concentration was quite different. In gas gland cells, approximately 75 µmol l^{-1} cytochalasin B would be required to cause a 50% decrease in the rate of metabolism (Fig. 5B), whereas in isolated myocytes, 25 µmol l^{-1} cytochalasin B resulted in 45% inhibition. RBCs were much more sensitive to cytochalasin B, in that a 77% inhibition of glucose metabolism was caused by 25 µmol l^{-1} cytochalasin B.

Comparison of rates of glucose metabolism with biochemical indicators

Glucose metabolism, levels of *GLUT1* and *HKI* transcripts, and HK activity were assessed in the same populations of gas gland cells, myocytes and RBCs. GLUT1 protein levels were not assessed in this population of cells because of the proteases used in the digestive medium. Glucose metabolism was 12-fold higher in gas gland than in heart and 170-fold higher than in RBCs (Fig. 6A). The pattern of the relative quantity of *GLUT1* mRNA was similar to that of glucose metabolism, although the level of *GLUT1* mRNA between gas gland and heart was not significantly different (Fig. 6B). The level of *HKIa* mRNA was significantly higher in heart than in either gas gland cells or RBCs (Fig. 6C). *HKIb* mRNA was significantly higher (90-fold) in gas gland cells than in the other cell types. The activity of total HK was significantly different amongst all three tissues, with gas gland cells having the highest and RBCs the lowest levels (Fig. 6F). The HK activity pattern was similar in rank order to that of glucose metabolism.

GLUT1 protein – localization and quantification

The basic structure of the total gas gland tissue was first assessed with standard haematoxylin and eosin staining (Fig. 7A,B). Examination at 40- and 400-fold magnification revealed gas gland cells and the rete mirabile. Immunohistochemical staining of 7 µm gas gland frozen sections with a mouse monoclonal anti-GLUT1 antibody, developed using red alkaline phosphatase substrate, showed that GLUT1 staining was confined to the glandular cells rather than the rete areas (Fig. 7C). No red staining was noted with an isotype-matched negative control antibody (Fig. 7C, inset). Sections were also stained for periodic acid–Schiff (PAS) and Oil-Red-O to detect glycoproteins and lipids/fats, respectively (not shown). The spaces encircled by the heavy GLUT1 staining were negative for PAS and Oil-Red-O stain.

Protein from lysates of gas gland, heart and RBCs was quantified, separated by SDS-PAGE and analysed for GLUT1 expression by western blot. GLUT1 western blot signal of Atlantic cod samples was compared to the signal of a primate retinal endothelial cell line that showed two main bands at 42 and 46 kDa, and a minor band of 52 kDa (Fig. 8A). Gas gland samples displayed one major band of 52 kDa, corresponding to the predicted molecular mass of GLUT1 (Hall et al., 2004), and a minor band of 43 kDa, while heart tissue presented a similar band pattern but the 52 kDa band was of lower intensity. The GLUT1 western blot displayed a very low signal in RBCs even with three times the amount of protein loaded (450 µg versus 150 µg). Coomassie Blue staining of tissues from two different animals revealed similar overall protein amounts in gas gland (50 µg) and heart (50 µg) sample sets, while the amount in

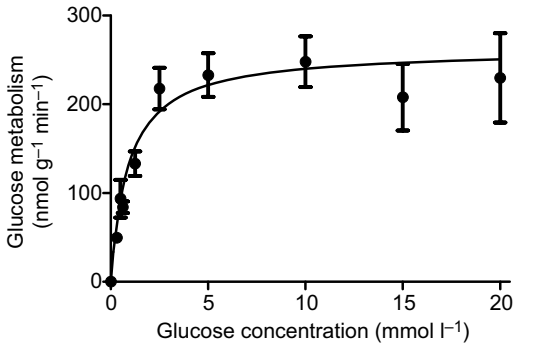

Fig. 3. Glucose metabolism by gas gland cells isolated from Atlantic cod at different concentrations of extracellular glucose. Cells were incubated in glucose for 2 h at 8°C. Sample sizes for the different concentrations of glucose (mmol l^{-1}) were as follows: 0, *N*=9; 0.3125, *N*=4; 0.5, *N*=5; 0.625, *N*=4; 1.25, *N*=4; 2.5, *N*=9; 5.0, *N*=9; 10, *N*=9; 15, *N*=4; and 20, *N*=4.

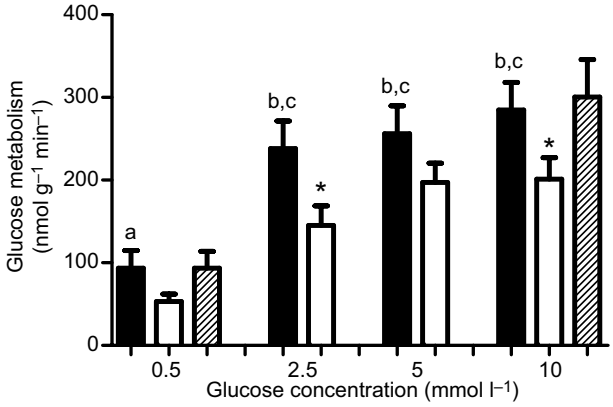

Fig. 4. Effect of cytochalasin B on glucose metabolism by gas gland cells isolated from Atlantic cod. Cells were incubated in 25 µmol l^{-1} cytochalasin B in the presence of four different concentrations of extracellular glucose (0.5, 2.5, 5 and 10 mmol l^{-1}). Filled bars, control (no cytochalasin B); open bars, plus cytochalasin B in DMSO; hatched bars, plus DMSO. *N*=5. A repeated measures ANOVA followed by Tukey's test was used to assess statistical significance. For simplicity, letters refer to control conditions only, where values sharing a common letter are not significantly different. Significant differences between control and cytochalsin B-treated preparations at the same extracellular glucose concentration are indicated with an asterisk.

Journal of Experimental Biology (2016) 219, 2763-2773 doi:10.1242/jeb.141721

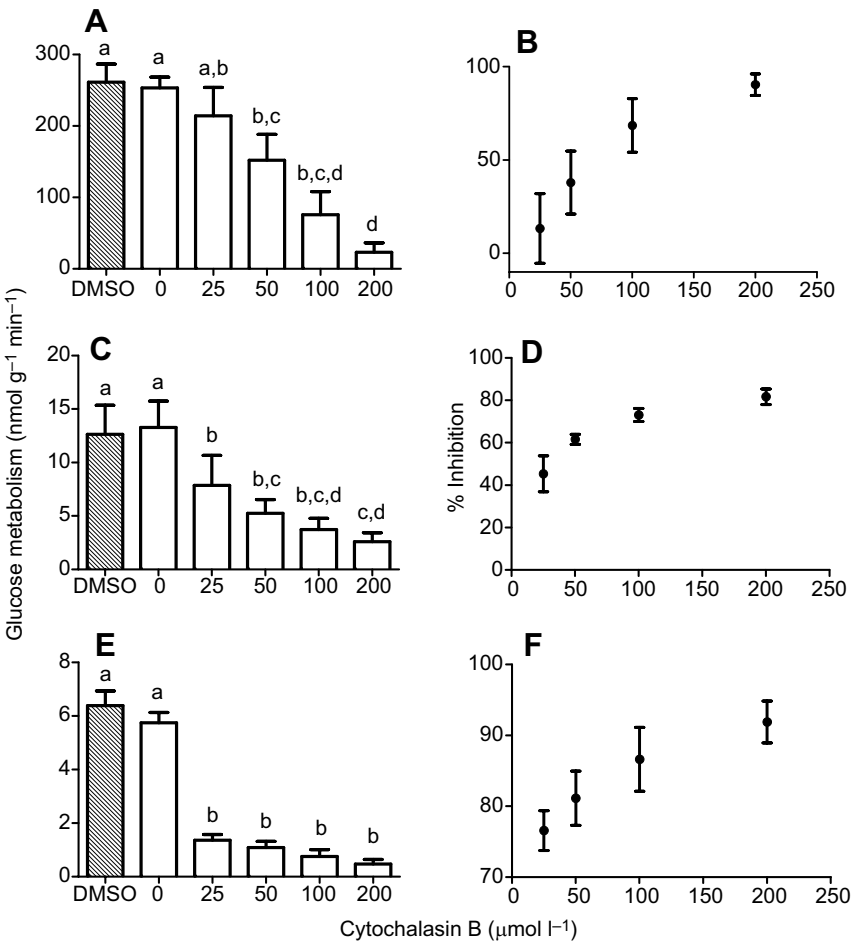

Fig. 5. Effect of increasing concentrations of cytochalasin B on glucose metabolism by cells isolated from Atlantic cod. Cells were incubated in 5 mmol l^{-1} glucose at 8°C for 2 h. (A,B) Gas gland cells. (C,D) Myocytes. (E,F) Red blood cells (RBCs). Hatched bars represent glucose metabolism with DMSO only in the medium. *N*=4 in all cases with each tissue preparation being tested under all conditions. The small sample size prevented a statistical assessment of normality, which was assumed. A repeated measures ANOVA followed by Tukey's test was used to assess statistical significance. Values sharing a common letter are not significantly different.

RBC samples was significantly reduced despite loading twice as much protein (100 µg; Fig. 8B). The reduced abundance of proteins in RBCs in this molecular mass range displayed by the Coomassie Blue-stained SDS-PAGE gel in Fig. 8B is probably associated with the high abundance of haemoglobin in these cells. The prominence of haemoglobin in RBCs in other species (95% of total cytosolic protein) is known to impede the detection of low abundance proteins (Bhattacharya et al., 2007). The qualitative results based on two animals suggest much higher levels of the 52 kDa band in the gas gland than in the heart, with even lower amounts in RBCs. This interpretation with respect to RBCs should be viewed with caution if the estimates of protein in these preparations are incorrect. Quantitative analysis of the 52 kDa GLUT1 western blot signal confirmed a twofold increase in gas gland over the heart when normalized to overall protein level (Fig. 9), while no significant difference was observed in the levels of the 43 kDa band (data not shown). In an analysis of a different set of animals, it was determined that levels of total soluble protein were similar in gas gland and heart, at 113±7 and 125±5 µg protein mg^{-1} cells, respectively (*N*=8 for both tissues); however, protein in RBCs was substantially higher at 434±31 µg protein mg^{-1} cell (*N*=8). When converted to RQ g^{-1} tissue, the level of GLUT1 protein in the gas gland was 2.3- and 33-fold higher than that in the heart and RBCs, respectively.

DISCUSSION

Methodology

Cells isolated from the gas gland and heart, as well as RBCs, were utilized as this approach allows time course measurements and multiple trial conditions with the same population of cells. Cells were isolated by standard techniques and preliminary experiments confirmed viability by dye exclusion. Maximal rates of glucose uptake were determined with radiolabelled 2-DG with well-established protocols used in fish heart and RBC studies (e.g. Becker et al., 2013; Tse and Young, 1990). This approach measures the initial rate of movement of 2-DG from the extracellular space into the cell against initially zero intracellular levels of 2-DG and provides insight into the mechanism of glucose transport. The uptake of 2-DG was shown to saturate at elevated concentrations of substrate, as expected for this type of experiment. Experiments were also conducted by tracking the production of ^3H_2O from [2-^{3}H]glucose. In this procedure, ^3H_2O is released from glycolysis in the conversion of G6P to fructose 6-phosphate, catalysed by phosphohexose isomerase. ^3H_2O is also released from the pentose phosphate shunt when 6-phosphogluconate is converted to ribulose 5-phosphate, catalysed by 6-phosphogluconate dehydrogenase (Hutton, 1972). The production of ^3H_2O was shown to be linear for at least 3 h and is considered to reflect rates of steady-state metabolism. The rate of metabolism was calculated based on the specific activity of extracellular glucose; however, the intracellular level of G6P that yields ^3H_2O by glycolysis is probably lower. In perfused rat hearts, the level of labelled G6P is 80% of that of extracellular glucose (Neely et al., 1972). The impact of substrate dilution on metabolites flowing through the pentose pathway is unknown. Therefore, our calculated rates of metabolism are likely to be small underestimates of true rates.

Journal of Experimental Biology (2016) 219, 2763-2773 doi:10.1242/jeb.141721

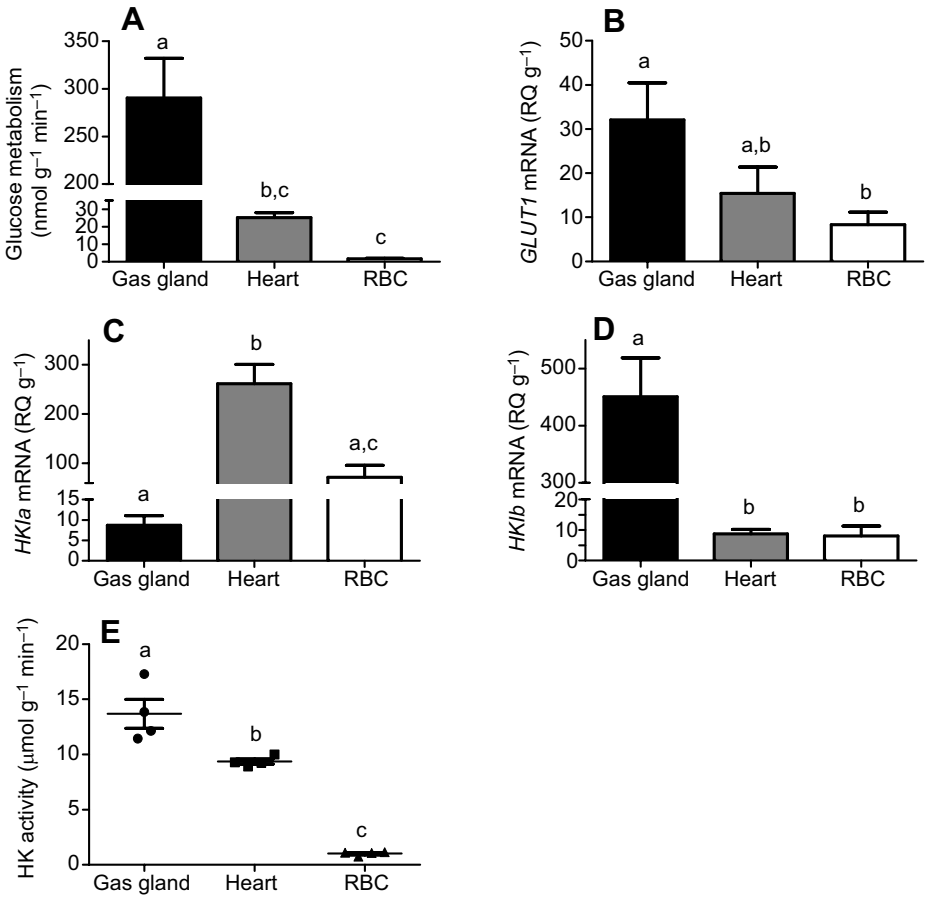

Fig. 6. Glucose metabolism, transcript levels and hexokinase (HK) activity in cells isolated from Atlantic cod. All parameters were determined on the same population of cells. (A) Glucose metabolism. (B) *GLUT1* mRNA. (C) *HKIa* mRNA. (D) *HKIb* mRNA. Transcript levels were normalized to tissue mass (RQ, relative quantity). (E) HK activity. *N*=8 in all cases except for HK activity, where *N*=4. In the case of HK activity, the small sample size prevented a statistical assessment of normality, which was assumed. Data were analysed by one-way ANOVA followed by Tukey's multiple comparison test. Values sharing a common letter are not significantly different.

Glucose metabolism by gas gland is higher than in heart or RBCs

The rate of glucose metabolism by gas gland cells at an extracellular glucose level of 5 mmol l^{-1} was very consistent across five separate experiments, with a mean value of 219±20 nmol g^{-1} min^{-1} (*N*=27). In the experiment in which glucose metabolism was measured in multiple tissues, the rate in gas gland cells was 12-fold higher than that in heart cells and 170-fold higher than that in RBCs. These values represent basal rates of metabolism. Although an earlier study showed catecholamines could stimulate lactate production by isolated pieces of Atlantic cod gas gland tissue (Ewart and Driedzic, 1990), treatment of isolated cells in the current experiment with isoproterenol did not result in an increase in the rate of glucose metabolism (data not shown). The gas gland in other species has glycogen deposits (Jasinski and Kilarski, 1969; Morris and Albright, 1975). It is possible that catecholamine stimulation results in the mobilization of glycogen reserves without an increase in extracellular glucose utilization.

Glucose is directed towards lactate production

The initial linearity study for the production of ^3H_2O from [2-^{3}H] glucose showed rates of 163 and 437 nmol g^{-1} cells min^{-1} for glucose metabolism and lactate production, respectively.

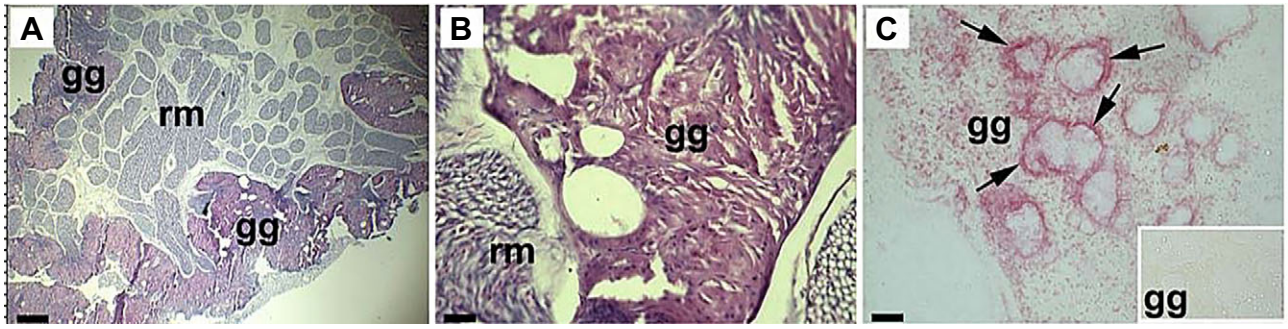

Fig. 7. Atlantic cod gas gland GLUT1 expression by immunohistochemistry. (A) Haematoxylin and eosin staining of a 7 µm frozen section of gas gland; rm, rete mirabile; gg, gas gland; scale bar, 150 µm. (B) Haematoxylin and eosin staining of a 7 µm frozen section of gas gland; scale bar, 15 µm. (C) Immunohistochemical staining of a 7 µm gas gland frozen section with a mouse monoclonal anti-GLUT1 antibody, developed using red alkaline phosphatase substrate. Red areas represent GLUT1 expression. The areas of heaviest GLUT1 staining appear to be located around putative tissue spaces and are indicated by arrows. The inset shows immunohistochemical staining of a 7 µm gas gland frozen section (identical to that in the main panel) with an isotype-matched negative control antibody. No red staining was detected. Scale bar, 15 µm.

Journal of Experimental Biology (2016) 219, 2763-2773 doi:10.1242/jeb.141721

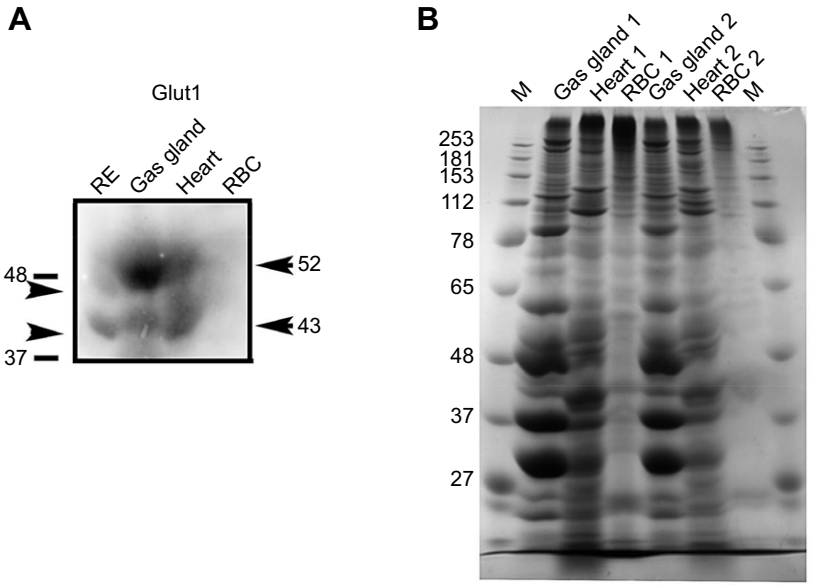

Fig. 8. GLUT1 molecular mass and tissue level approximation in Atlantic cod gas gland, heart and RBCs. (A) GLUT1 western blot signals in Atlantic cod tissues compared with those for a primate retinal endothelial (RE) cell line positive control (100 µg), which shows two main bands of 42 and 46 kDa (arrowheads) and a minor band of 52 kDa. Gas gland and heart samples (150 µg) from Atlantic cod displayed 43 and 52 kDa bands (arrows) while the signal in RBCs (450 µg) was not clear. (B) Coomassie Blue staining of two sets (1 and 2) of tissues revealed similar overall protein amounts in gas gland (50 µg) and heart (50 µg) sample sets, while the amount in RBC samples was significantly reduced despite loading twice as much protein (100 µg). M: molecular mass markers (kDa), indicated on the left-hand side.

The ratio of lactate production to glucose metabolism was not significantly different from 2 (2.76±0.49). Given that there will be some isotope dilution, which will lead to underestimation of the rate of glucose metabolism, the true ratio of lactate production to glucose metabolism will be even closer to 2.

As such, most of the extracellular glucose is utilized to support lactate production. The methodology does not reveal the relative rates of metabolism through glycolysis or the pentose phosphate pathway. The conclusion that all of the glucose is converted to lactate plus CO_2 (via the pentose shunt) is consistent with observations that in gas gland of Atlantic cod and other species, there are few and/or poorly developed mitochondria and low activities of enzymes of the citric acid cycle and cytochrome oxidase (Copeland, 1969; Jasinski and Kilarski, 1969; Morris and Albright, 1975; Boström et al., 1972; Ewart and Driedzic, 1990; Pelster and Scheid, 1991; Walsh and Milligan, 1993).

Dependence upon GLUT1 and facilitative glucose diffusion

Glucose utilization by gas gland cells is very much dependent upon facilitated diffusion. This contention is based upon the following observations. The uptake of 2-DG saturates at an extracellular concentration of less than 0.5 mmol l^{-1}, consistent with a transport mechanism (i.e. transport protein saturation). Glucose metabolism was 90% inhibited by cytochalsin B at a concentration of 200 µmol l^{-1}. The usual concentration of cytochalasin B utilized in studies of this nature with fish cells is 10–25 µmol l^{-1} (e.g. Tse and Young, 1990; Becker et al., 2013; Driedzic et al., 2014). At a cytochalasin B concentration of 25 µmol l^{-1}, glucose metabolism was inhibited by 13%, 45% and 77% in the gas gland, heart and RBCs, respectively. Cytochalasin B impairs glucose transport by binding to GLUT1 on the inner membrane and is a competitive inhibitor of glucose efflux (Silverman, 1991). The much higher levels of cytochalasin B required to inhibit glucose metabolism in gas gland than in heart or RBCs probably reflects a greater abundance of transport protein. GLUT1 protein is localized to the glandular cells and not the blood vessels, as evidenced by immunohistochemistry using a mouse monoclonal IgG2b anti-GLUT1 antibody. This finding is in keeping with *in situ* hybridization analysis of the gas gland in torafugu (Munakata et al., 2012). The lack of PAS and Oil-Red-O staining of putative extracellular spaces encircled by heavy GLUT1 staining suggests that these spaces were 'empty' and that the gas gland lumen might be continuous with air channels that penetrate the gas gland tissue, given that in Atlantic cod the gas gland resides within the swim bladder. This contention would have to be confirmed in further anatomical studies.

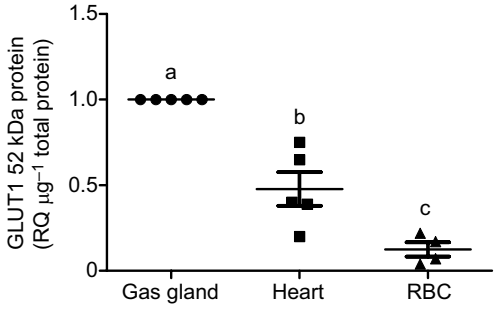

Fig. 9. Levels of 52 kDa GLUT1 protein relative to total protein. Data for individual animals were normalized to those for the gas gland. *N*=5 for gas gland and heart; *N*=4 for RBCs. In the case of RBCs, the small sample size prevented a statistical assessment of normality, which was assumed. Data were analysed by one-way ANOVA followed by Tukey's multiple comparison test. Values sharing a common letter are not significantly different.

GLUT1 is the predominant transcript of class I glucose transporter in Atlantic cod gas gland, heart and RBCs (Hall et al., 2014). In the gas gland, *GLUT1* mRNA accounts for 98% of the sum of *GLUT1–4* transcripts. Based on cDNA sequence, Atlantic cod *GLUT1* is predicted to encode a 489 amino acid protein with a molecular mass of 53.5 kDa (Hall et al., 2004). In the current study, western blotting showed a dominant band of 52 kDa, which is consistent with the predicted mass of the putative protein. There was also a minor 43 kDa band, which is possibly a breakdown product of the larger protein. The 52 kDa protein, which is likely to be the active protein, was 2.3- and 33-fold more abundant in the gas gland than in the heart and RBCs, respectively, when normalized to tissue mass. The pattern for the relative amounts of GLUT1 protein in the gas gland, heart and RBCs (1:2.3:33) is similar to the pattern for rates of glucose metabolism (1:12:170), suggesting that the amount of GLUT1 protein is associated with the capacity to utilize extracellular glucose as a metabolic fuel.

Importance of HKIb

Atlantic cod express two *HKI* paralogous transcripts that were previously named *HKIa* and *HKIb*; their putative protein sequences are 86% identical (Hall et al., 2009). HKI typically binds to mitochondria, where it is considered to deliver G6P to glycolysis and subsequently the citric acid cycle (Wilson, 2003; Calmettes et al., 2013). A specific 15 amino acid N-terminal domain is required for binding to the outer mitochondrial membrane (Gelb et al., 1992; Sui and Wilson, 1997). Although not supported by experimental evidence, in Atlantic cod, a substitution of leucine for isoleucine at site 7 in HKIb should prevent binding from occurring (Hall et al., 2004). Here, we showed that *HKIa* transcripts are more abundant in heart (30-fold higher) and RBCs (8-fold higher) than in gas gland. In contrast, *HKIb* transcripts in gas gland are 52-fold higher than in heart and 57-fold higher than in RBCs. This distribution is consistent with the high mitochondrial density typically found in heart and low mitochondrial density of gas gland cells (Copeland, 1969; Morris and Albright, 1975). The high rates of glucose metabolism leading to lactate production in the gas gland relative to the heart and RBCs appears to be associated with high transcript levels of *HKIb*, an unusual *HKI* paralogue that is predicted to encode a cytosolic protein. The HKII isoform moves freely from a mitochondrial binding site to the cytosol (Wilson, 2003; Calmettes et al., 2013) and is insulin sensitive (Mandarino et al., 1995; Wilson, 2003; Calmettes et al., 2013), similar to GLUT4 (Wood and Trayhurn, 2003; Mueckler and Thorens, 2013). Our previous attempts to clone Atlantic cod *HKII* were unsuccessful (Hall et al., 2009), and although *GLUT4* transcripts can be detected in Atlantic cod, these occur at very low levels relative to the other class I GLUTs. For instance, in heart, *GLUT4* transcript accounts for only 3% of the total *GLUT* transcripts (Hall et al., 2014). Recognizing that our inability to clone HKII does not in itself constitute proof of its absence, we suggest that Atlantic cod may have a relatively low dependence upon insulin-mediated glucose metabolism and that the role of HKII in this species is taken over by HKIb.

Maximal *in vitro* activity of HK was significantly higher in the gas gland than in the heart or RBCs. The activities are similar to those previously reported for the gas gland (Ewart and Driedzic, 1990) and heart (Hansen and Sidell, 1983) using similar methodologies. The measured activities will include contributions from all of the isoforms present and although the rank order of the rate of glucose metabolism and total HK activity across tissues is the same, there is no linear correlation between the two parameters. The maximal *in vitro* HK activity is substantially higher than the rate of metabolism. For instance, in the gas gland, glucose metabolism is 0.29 µmol g^{-1} cells min^{-1} compared with a maximal HK activity of 14 µmol g^{-1} cells min^{-1}. This suggests that HK activity could easily keep pace with glucose uptake; however, this point requires more detailed examination. In experiments with isolated cells exposed to physiological concentrations of the glucose analogue 2-DG, there were higher levels of intracellular 2-DG than 2-DGP, suggesting that rates of glucose entry may exceed phosphorylation under some conditions. The most likely explanation for the mismatch between glucose metabolism and HK activity is that the enzyme is very much inhibited *in situ* by G6P as it is in other tissues (Rodnick et al., 1997; Wilson, 2003). Regardless, it appears that high rates of glucose utilization are associated with high *in vitro* levels of HK activity.

Conclusions

The current study confirms that rates of steady-state glucose metabolism are higher in the gas gland followed by the heart and RBCs of Atlantic cod. Essentially all of the extracellular glucose metabolized by the gas gland is converted to lactate. This is consistent with the low aerobic capacity of gas glands despite functioning in a hyperoxic microenvironment. High rates of glucose metabolism are dependent upon facilitated glucose transport via high levels of GLUT1 protein, which is 2.3- and 33-fold more abundant in the gas gland than in the heart and RBCs, respectively. The protein is present in Atlantic cod gas gland and has a molecular mass of 52 kDa as predicted from its deduced amino acid sequence. Once glucose enters the cell it is phosphorylated by HKIb. This HKI paralogue is unusual in that it has a substitution in the N-terminal domain that may prevent it from binding to mitochondria. During steady-state metabolism, the rate of glucose uptake must equal the rate of phosphorylation. The gas gland has high *in vitro* activity levels of HK that allows a matching of the first two steps in glucose utilization.

Acknowledgements

The authors thank D. Boyce (Department of Ocean Sciences) for the supply of Atlantic cod and Dr Matthew Rise (Department of Ocean Sciences) for use of the ViiA 7 Real-Time PCR system.

Competing interests

The authors declare no competing or financial interests.

Author contributions

K.A.C., C.E.S., J.R.H., R.L.G., H.P. and A.R. were responsible for the execution of the studies. K.A.C., C.E.S., J.R.H., R.L.G. and H.P. reviewed drafts of the manuscript. W.R.D. was responsible for experimental design, interpretation of the findings and drafting of the article.

Funding

This work was supported by the Natural Sciences and Engineering Research Council of Canada (W.R.D.); the Canadian Institutes of Health Research (FRN-123888; R.L.G. and H.P.); the Research and Development Corporation of Newfoundland and Labrador (W.R.D., R.L.G. and H.P.); and by an infrastructure grant from the Canada Foundation for Innovation (7411; R.L.G. and H.P.). W.R.D. holds the Canada Research Chair (Tier 1) in Marine Bioscience.

References

Becker, T. A., DellaValle, B., Gesser, H. and Rodnick, K. J. (2013). Limited effects of exogenous glucose during severe hypoxia and a lack of hypoxia-stimulated glucose uptake in isolated rainbow trout cardiac muscle. *J. Exp. Biol.* **216**, 3422-3342.

Bhattacharya, D., Mukhopadhyay, D. and Chakrabarti, A. (2007). Hemoglobin depletion from red blood cell cytosol reveals new proteins in 2-D gel-based proteomics study. *Proteomics Clin. Appl.* **1**, 561-564.

Boström, S.-L., Fänge, R. and Johansson, R. G. (1972). Enzyme activity patterns in gas gland tissue of the swimbladder of the cod (*Gadus morrhua*). *Comp. Biochem. Physiol.* **43B**, 473-478.

Calmettes, G., John, S. A., Weiss, J. N. and Ribalet, B. (2013). Hexokinase-mitochondrial interactions regulate glucose metabolism differentially in adult and neonatal cardiac myocytes. *J. Gen. Physiol.* **142**, 425-436.

Chen, L.-Q., Cheung, L. S., Feng, L., Tanner, W. and Frommer, W. B. (2015). Transport of sugars. *Annu. Rev. Biochem.* **84**, 865-894.

Copeland, D. E. (1969). Fine structural study of gas secretion in the physoclistous swim bladder of *Fundulus heteroclitus* and *Gadus callarias* and in the euphysoclistous swim bladder of *Opsanus tau*. *Z. Zellforsch. Mikrosk. Anat.* **93**, 305-331.

Driedzic, W. R., Clow, K. A. and Short, C. E. (2013). Glucose uptake and metabolism by red blood cells from fish with different extracellular glucose levels. *J. Exp. Biol.* **216**, 437-446.

Driedzic, W. R., Clow, K. A. and Short, C. E. (2014). Extracellular glucose can fuel metabolism in red blood cells from high glycemic Atlantic cod (*Gadus morhua*) but not low glycemic short-horned sculpin (*Myoxocephalus scorpius*). *J. Exp. Biol.* **217**, 3797-3804.

Ewart, H. S. and Driedzic, W. R. (1990). Enzyme activity levels underestimate lactate production rates in cod (*Gadus morhua*) gas gland. *Can. J. Zool.* **68**, 193-197.

Gelb, B. D., Adams, V., Jones, S. N., Griffin, L. D., MacGregor, G. R. and McCabe, S. (1992). Targeting of hexokinase 1 to liver and hepatoma mitochondria. *Proc. Natl. Acad. Sci. USA* **89**, 202-206.

Hall, J. R., MacCormack, T. J., Barry, C. A. and Driedzic, W. R. (2004). Sequence and expression of a constitutive, facilitated glucose transporter (GLUT1) in Atlantic cod *Gadus morhua*. *J. Exp. Biol.* **207**, 4697-4706.

Hall, J. R., Short, C. E., Petersen, L. H., Stacey, J., Gamperl, A. K. and Driedzic, W. R. (2009). Expression levels of genes associated with oxygen utilization, glucose transport and glucose phosphorylation in hypoxia exposed Atlantic cod (*Gadus morhua*). *Comp. Biochem. Physiol. D* **4**, 128-138.

Hall, J. R., Clow, K. A., Short, C. E. and Driedzic, W. R. (2014). Transcript levels of class I GLUTs within individual tissues and the direct relationship between GLUT1 expression and glucose metabolism in Atlantic cod (*Gadus morhua*). *J. Comp. Physiol. B* **184**, 483-496.

Hansen, C. A. and Sidell, B. D. (1983). Atlantic hagfish cardiac muscle: metabolic basis of tolerance to anoxia. *Am. J. Physiol.* **244**, R356-R362.

Hutton, J. J. (1972). Radiometric micromethod for quantitation of glucose utilization by the erythrocyte. *Anal. Biochem.* **45**, 577-584.

Jasiński, A. and Kilarski, W. (1969). On the fine structure of the gas gland in some fishes. *Z. Zellforsch. Mikrosk. Anat.* **102**, 333-356.

Mandarino, L. J., Printz, R. L., Cusi, K. A., Kinchington, P., O'Doherty, R. M., Osawa, H., Sewell, C., Consoli, D. K., Granner, D. K. and DeFronzo, R. A. (1995). Regulation of hexokinase II and glycogen synthase mRNA, protein, and activity in human muscle. *Am. J. Physiol.* **269**, E701-E708.

Morris, S. M. and Albright, J. T. (1975). The ultrastructure of the swimbladder of the toadfish, *Opsanus tau* L. *Cell Tiss. Res.* **164**, 85-104.

Mueckler, M. and Thorens, B. (2013). The SLC (GLUT) family of membrane transporters. *Mol. Aspects Med.* **34**, 121-138.

Munakata, K., Ookata, K., Doi, H., Baba, O., Terashima, T., Hirose, S. and Kato, A. (2012). Histological demonstration of glucose transporters, fructose-1,6-bisphosphatase, and glycogen in gas gland cells of the swimbladder: Is a metabolic futile cycle operating? *Biochem. Biophys. Res. Comm.* **417**, 564-569.

Neely, J. R., Denton, R. M., England, P. J. and Randle, P. J. (1972). The effects of increased heart work on the tricarboxylate cycle and its interactions with glycolysis in the perfused rat heart. *Biochem. J.* **128**, 147-159.

Nilsson, S. (2009). Nervous control of fish swimbladders. *Acta Histochem.* **111**, 176-184.

Paradis, H., Islam, T., Tucker, S., Tao, L., Koubi, S. and Gendron, R. L. (2008). Tubedown associates with cortactin and controls permeability of retinal endothelial cells to albumin. *J. Cell Sci.* **121**, 1965-1972.

Pelster, B. (1997). Buoyancy at depth. In *Deep-Sea Fish, Fish Physiology*, Vol. 16 (ed. D. Randall and A. P. Farrell), pp. 185-237. San Diego, CA: Academic Press.

Pelster, B. (2004). pH regulation and swimbladder function in fish. *Resp. Physiol. Neurobiol.* **144**, 179-190.

Pelster, B. (2015). Swimbladder function and the spawning migration of the European eel *Anguilla anguilla*. *Front. Physiol.* **5**, 1-9.

Pelster, B. and Scheid, P. (1991). Activities of enzymes for glucose catabolism in the swimbladder of the European eel *Angulla anguilla*. *J. Exp. Biol.* **156**, 207-213.

Pelster, B. and Scheid, P. (1993). Glucose metabolism of the swimbladder tissue of the European eel *Anguilla Anguilla*. *J. Exp. Biol.* **185**, 169-178.

Pelster, B., Kobayashi, H. and Scheid, P. (1989). Metabolism of the perfused swimbladder of the European eel: oxygen, carbon dioxide, glucose, and lactate balance. *J. Exp. Biol.* **144**, 495-506.

Pelster, B., Hicks, J. and Driedzic, W. R. (1994). Contribution of the pentose phosphate shunt to the formation of CO2 in swimbladder tissue of the eel. *J. Exp. Biol.* **197**, 119-128.

Pfaffl, M. W. (2001). A new mathematical model for relative quantification in real-time PT-PCR. *Nucleic Acids Res.* **29**, e45.

Rodnick, K. J., Bailey, J. R., West, J. L., Rideout, A. and Driedzic, W. R. (1997). Acute regulation of glucose uptake in cardiac muscle of the American eel, *Anguilla rostrata*. *J. Exp. Biol.* **200**, 2871-2880.

Silverman, M. (1991). Structure and function of hexose transporters. *Annu. Rev. Biochem.* **60**, 757-794.

Sui, D. and Wilson, J. E. (1997). Structural determinants for the intracellular localization of the isozymes of mammalian hexokinase: intracellular localization of fusion constructs incorporating structural elements from the hexokinase isozymes and the green fluorescent protein. *Arch. Biochem. Biophys.* **345**, 111-125.

Tse, C.-M. and Young, J. D. (1990). Glucose transport in fish erythrocytes: variable cytochalasin-B-sensitive hexose transport activity in the common eel (*Anguilla japonica*) and transport deficiency in the paddyfield eel (*Monopterus albus*) and rainbow trout (*Salmo gairdneri*). *J. Exp. Biol.* **148**, 367-383.

Umezawa, T., Kato, A., Ogoshi, M., Ookata, K., Munakata, K., Yamamoto, Y., Islam, Z., Doi, H., Romero, M. F. and Hirose, S. (2012). O_2-filled swimbladder employs monocarboxylate transporters for the generation of O_2 by lactate-induced root effect hemoglobin. *PLoS ONE* **7**, e34579.

Walsh, P. J. and Milligan, L. (1993). Roles of buffering capacity and pentose phosphate pathway activity in the gas gland of the gulf toadfish Opanus beta. *J. Exp. Biol.* **176**, 311-316.

Wilson, J. E. (2003). Isozymes of mammalian hexokinase: structure, subcellular localization and metabolic function. *J. Exp. Biol.* **206**, 2049-2057.

Wood, I. S. and Trayhurn, P. (2003). Glucose transporters (GLUT and SGLT): expanded families of sugar transport proteins. *Br. J. Nutr.* **89**, 3-9.